UDC 546.05+546.302+621.355.82

N.O. Chorna [a], V.M. Kordan [a], A.M. Mykhailevych [a], O.Ya. Zelinska [a], A.V. Zelinskiy [a], K. Kluziak [b], R.Ya. Serkiz [a], V.V. Pavlyuk [a, b]

ELECTROCHEMICAL HYDROGENATION, LITHIATION AND SODIATION OF THE $GdFe_{2-x}M_x$ AND $GdMn_{2-x}M_x$ INTERMETALLICS

[a] Ivan Franko National University of Lviv, Lviv, Ukraine

[b] Jan Długosz University of Czestochowa, Czestochowa, Poland

Electrochemical hydrogenation, lithiation and sodiation of the phases $GdFe_{2-x}M_x$ and $GdMn_{2-x}M_x$ (M=Mn, Co, Ni, Zn, and Mg) and the influence of doping components on electrochemical characteristics of electrode materials on their basis were studied using X-ray powder diffraction method, scanning electron microscopy, energy dispersive X-ray analysis, X-ray fluorescent spectroscopy, cyclic voltammetry and electrochemical impedance spectroscopy. Phase analysis showed a simple correspondence between unit cell parameters of the phases and atomic radii of doping elements. Electrode materials based on $GdFe_2$ and $GdMn_2$ doped with 2 at.% of Co, Ni and Mg demonstrated better hydrogen sorption properties than those doped with Mn and Zn. Corrosion resistance of the doped electrodes was also better than of the binary analogues (e.g. corrosion potential of the $GdFe_2$-based electrode was −0.162 V whereas that of $GdFe_{1.96}Ni_{0.04}$ was −0.695 V). The capacity parameters were increased in the following ranges: Zn<Mn<Mg<Co<Ni and Zn<Fe<Mg<Co<Ni for $GdFe_{2-x}M_x$ and $GdMn_{2-x}M_x$, respectively. After fifty cycles of charge/discharge, we observed the changes in surface morphology and composition of the electrode samples. In the structure of studied Laves type phases with $MgCu_2$-type structure, the most suitable sites for hydrogen atoms are tetrahedral voids 8*a*. During lithiation and sodiation of the phases, the atoms of the M-component of the structure are replaced by the atoms of lithium, and the atoms of gadolinium are replaced by the atoms of sodium. This difference in interaction is due to the difference in atomic sizes of the atoms. No insertion of lithium or sodium into the structural voids of the phases was observed.

Keywords: solid solution, electrochemical hydrogenation, lithiation and sodiation, Ni-MH battery, Li-ion battery, Na-ion battery.

DOI: 10.32434/0321-4095-2021-135-2-139-149

Introduction

The ability of multicomponent alloys based on rare earth and transition metals to absorb/desorb hydrogen enables their use for hydrogen storage and as electrode materials in metal-hydride batteries. Intermetallic compounds with certain composition and type of structures like RM_2 (Laves phases), RM_3 ($PuNi_3$-type or $CeNi_3$-type structure), RM_5 ($CaCu_5$-type structure), and R_2M_{17} (Th_2Ni_{17}-type or Th_2Zn_{17}-type structure), where R is rare earth and M is 3d-transition element, or their ternary derivatives can demonstrate this behavior, and only some of them can reversibly absorb/desorb hydrogen at room temperature.

Investigation of RM_2-phases, which crystallize as cubic C15 type Laves phases (space group Fd-3m), generally consisted in studying their magnetic properties and determining magnetic structure. Some of the phases can absorb ~5 H/f.u. and form hydrides. Hydrogenation of the phase ErFeMn did not cause the change of its crystal structure [1], but led to large expansion of the unit cell volume. However, a large amount of hydrogen can cause a structural transformation of the initial compounds [2,3]. The binary compound $GdMn_2$ orders magnetically at about 100 K, and a sudden increase in the unit cell volume by about 0.4% is observed at this temperature [4]. This compound readily absorbs hydrogen, and Zukrowski et al. [2] presented complex structural and magnetic

experimental results concerning $GdMn_2H_x$ hydrides. Mori et al. [5] showed that hydrides $GdFe_2H_{3.3}$ and $GdFe_2H_{4.3}$ prepared by gas hydrogenation are non-collinear ferromagnets. Increasing the hydrogen content reduces the magnetic ordering temperature from 469 K to 360 K and raises the compensation temperature from 45 to 202 K. Hydrogenation was also used to prepare magnetic amorphous hydrides: if a large amount of hydrogen was absorbed, the crystal structure was destroyed and amorphous materials with ferromagnetic properties were obtained. Amorphization of the samples can also occur during electrochemical processes when using high current densities [6,7]. Doping of the Laves phases RM_2 with other elements improves their water-sorption, magnetic and electrochemical properties [8,9,10]. Our previous study of the Gd–Fe–Zn system has showed that doping of the binary compounds GdZn and $GdZn_2$ with iron improved the electrochemical properties of electrode samples, increased the amount of intercalated hydrogen and enhanced corrosion resistance of doped samples in an alkaline medium [11].

The aim of this research was to investigate the binary intermetallics $GdMn_2$ and $GdFe_2$ doped with some 3d-elements (manganese, cobalt, nickel, and zinc) and s-element (magnesium) with the purpose of their electrochemical hydrogenation, lithiation and sodiation. We also established the influence of dopants on electrochemical and sorption characteristics of the electrode materials based on these phases.

Experimental

Synthesis of the alloys was carried out by arc melting of the pure metals (nominal purity more than 99.9 wt.%) under a purified argon atmosphere. The samples were sealed in evacuated silica ampoules and annealed at 500^0C for two months with final quenching in cold water. X-ray powder diffraction (XRD) of the alloys was carried out using a DRON-2.0M diffractometer (FeK_α-radiation, $20^0 \le 2\theta \le 100^0$). The unit cell parameters were refined by least-squares method using the LATCON program [12]. The morphology of the samples surfaces and compositions of their grains were studied by scanning electron microscopy (SEM) and energy dispersive X-ray analysis (EDX) using electron microscopes REMMA-102-02 and Tescan Vega3 LMU with Oxford Instruments EDX-system. X-ray fluorescent spectrometer ElvaX Pro was used to determine an integral composition of powdered alloys before and after electrochemical processes. Electrochemical characteristics of the phases were studied in two- and three-electrode «Swagelok»-type cells. We used the powder of the synthesized alloys with a mass of ~0.3 g as an anode material. It was mixed with an electrolyte to obtain a homogeneous mass and then filled the space of an anode area of the battery. We used a mixture of nickel (II) hydroxide (α- and β-modifications) and graphite in the ratio of 9:1, respectively, as a cathode material. Graphite was added to improve conductivity of the samples. The anode and cathode spaces were separated by a separator made of pressed cellulose and impregnated with electrolyte (6 M solution of KOH). All samples were tested in galvanostatic mode (galvanostat MTech G410-2). The charge process of the battery prototypes was carried out at 0.5 mA cm^{-2}, and the discharge process was carried out at 0.2 mA cm^{-2}. The hydrogen capacity of the electrodes was determined according to Faraday's law. The electrochemical reactions that occurred on the electrodes can be presented by the following scheme:

$$GdFe_{2-x}M_x + zH_2O + z\bar{e} \underset{\text{discharge}}{\overset{\text{charge}}{\rightleftarrows}} \rightleftarrows GdFe_{2-x}M_xH_z + zOH^-,$$

$$Ni(OH)_2 + zOH^- \underset{\text{discharge}}{\overset{\text{charge}}{\rightleftarrows}} \rightleftarrows NiOOH + zH_2O + z\bar{e}.$$

Cyclic voltammetry and electrochemical impedance spectroscopy was performed using a three-electrode cell and potentiostat-galvanostat CH Instruments (Austin, TX, USA). Negative electrodes for this purpose were prepared by mixing 80 wt.% of powdered alloys as active materials, 10 wt.% of black carbon (electronically conductive additive) and 10 wt.% of PVDF binder in an agate mortar. The electrochemical investigations were conducted by means of «Swagelok»-type cells. $Ni/Ni(OH)_2$ or Hg/HgO were used as a reference electrode. Potential scan rate from the cathodic direction towards the anodic one was 10 mV s^{-1}. The lithium-ion cells contain $GdFe_{2-x}M_x$ electrode as a working electrode with Li reference and $LiCoO_2$ counter electrodes. The sodium-ion cells contain Na as a reference and Na_xCoO_2 as counter electrodes, respectively. The ethylencarbonate/dimethylcarbonate nonaqueous electrolyte containing Li^+ or Na^+ ions was used. The anode and cathode were separated by Celgard 2320 separator impregnated with electrolyte.

Results and discussion

X-ray diffraction studies and phase analysis of alloys

Intermetallic compounds $GdMn_2$ and $GdFe_2$

($MgCu_2$-type, space group Fd-3m, Pearson code cF24) can solve the third component forming solid solutions of substitution. The main purpose of alloying these binary compounds with 3d- and s-elements was improving their electrochemical, corrosion and hydrogen sorption properties. In this study, we used 2 at.% of Mn, Co, Ni, Zn and Mg as dopants. Investigation of gas and electrochemical hydrogenation of magnesium doped with lithium and aluminium is described elsewhere [13,14].

According to the results of X-ray powder diffraction, all of the synthesized phases before hydrogenation crystallize in the expected type of structure with negligible impurities of other phase ($PuNi_3$-type structure in case of $GdFe_{2-x}M_x$ solid solutions or Gd_6Mn_{23}-type structure in case of $GdMn_{2-x}M_x$ solid solutions). After electrochemical hydrogenation, all samples showed an increase in unit cell parameters as compared with the initial alloys due to the formation of hydrides of inclusion (Table 1). There is also a clear dependence of the unit cell parameters of the synthesized phases and atomic radii of dopants (Fig. 1). In case of Mg, a covalent radius is used for better correlation. During electrochemical hydrogenation, we observed partial amorphization of the electrode materials, as evidenced by the appearance of an amorphous halo at a small angle range and extended peak profiles on XRD powder patterns of $GdFe_2$ and $GdMn_2$ after hydrogenation. Sometimes, the interaction of the material surface and electrolyte led to the changes in the morphology and composition of the grains which we confirmed by EDX-analysis (Fig. 2). The corrosion resistant dopants, such as Co and Ni, decrease leaching the surface (Fig. 2, c–f). Integral composition of the electrode materials based on

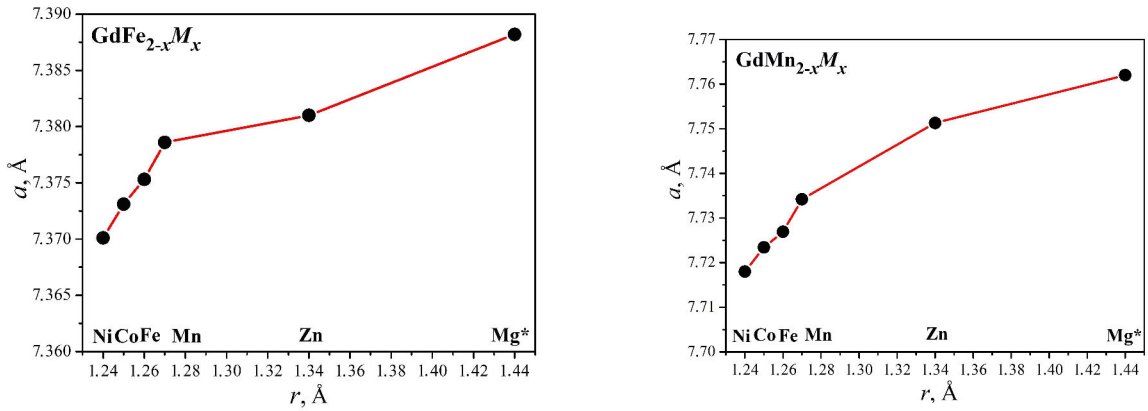

a **b**

Fig. 1. Dependence of unit cell parameter a on atomic radii r of dopant (* – a covalent radius of Mg is used)

Fig. 2. SEM images of the electrode materials based on the studied alloys before (a, c, e, g) and after (b, d, f, h) electrochemical hydrogenation (integral composition of the grains is given in parentheses)

Table 1

Unit cell parameters for $GdFe_{2-x}M_x$ and $GdMn_{2-x}M_x$ alloys before and after hydrogenation

Nominal composition of alloy	Unit cell parameters				
	before hydrogenation		after hydrogenation		ΔV/V, %
	a, Å	V, Å^3	a, Å	V, Å^3	
$GdFe_2$	7.376(2)	401.4(3)	7.399(1)	405.0(1)	0.89
$GdFe_{1.94}Zn_{0.06}$	7.3796(2)	401.98(4)	7.409(1)	406.8(2)	1.22
$GdFe_{1.94}Ni_{0.06}$	7.3689(3)	400.15(5)	7.3840(8)	402.6(1)	0.61
$GdFe_{1.94}Co_{0.06}$	7.3744(7)	401.0(3)	7.3824(8)	402.3(1)	0.32
$GdFe_{1.94}Mn_{0.06}$	7.3786(4)	401.72(7)	7.393(1)	404.0(2)	0.57
$GdFe_{1.94}Mg_{0.06}$	7.3882(9)	403.3(1)	7.424(1)	409.2(2)	1.46
$GdMn_2$	7.7362(9)	463.0(2)	7.759(1)	467.1(2)	0.88
$GdMn_{1.94}Zn_{0.06}$	7.7504(6)	465.5(1)	7.7664(9)	468.4(2)	0.62
$GdMn_{1.94}Ni_{0.06}$	7.718(2)	459.7(4)	7.751(3)	465.6(6)	1.28
$GdMn_{1.94}Co_{0.06}$	7.7234(7)	460.7(1)	7.758(1)	466.9(2)	1.35
$GdMn_{1.94}Fe_{0.06}$	7.7269(8)	461.3(1)	7.739(2)	463.5(3)	0.48
$GdMn_{1.94}Mg_{0.06}$	7.7579(5)	466.92(9)	7.779(3)	470.7(5)	0.81

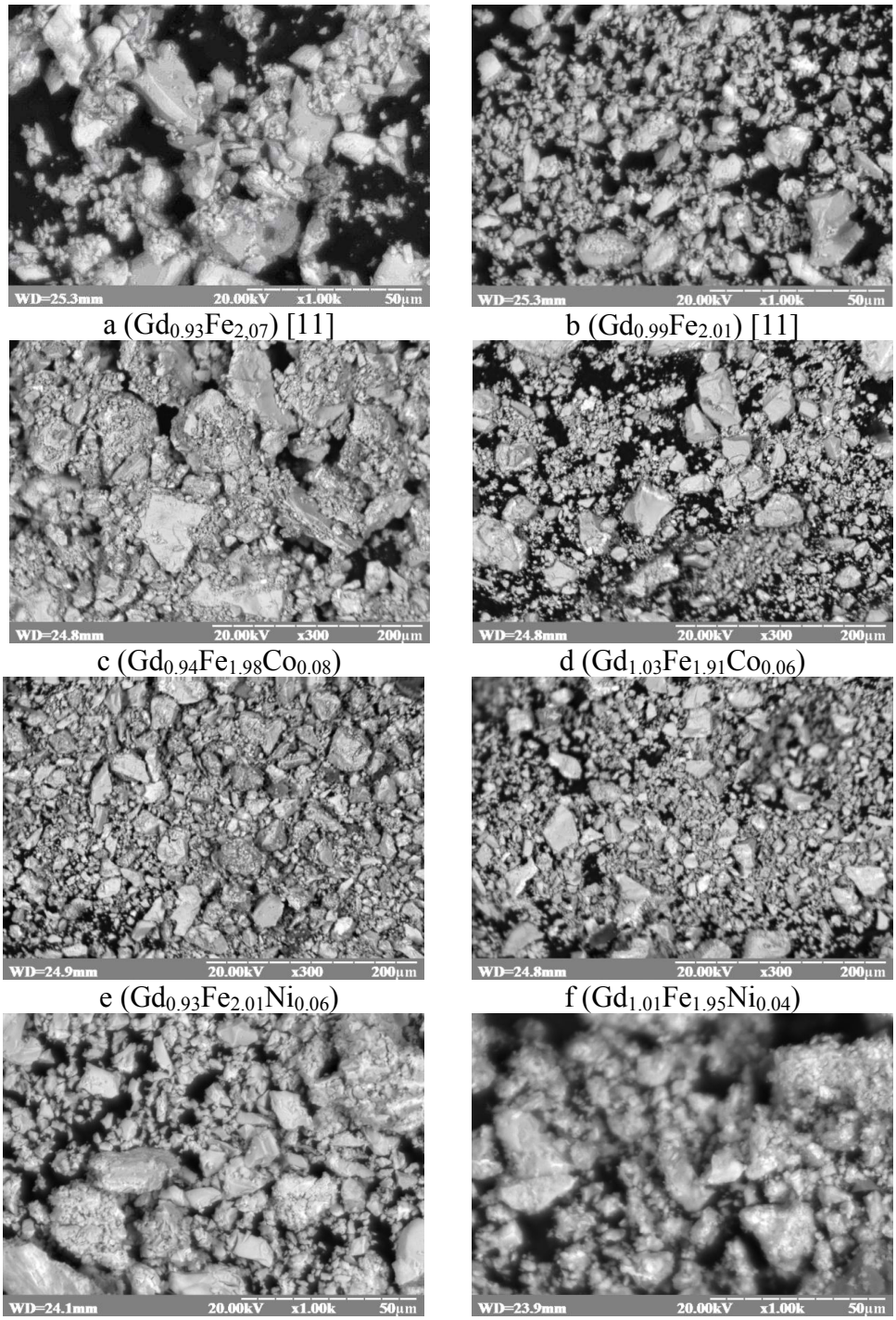

a ($Gd_{0.93}Fe_{2.07}$) [11]

b ($Gd_{0.99}Fe_{2.01}$) [11]

c ($Gd_{0.94}Fe_{1.98}Co_{0.08}$)

d ($Gd_{1.03}Fe_{1.91}Co_{0.06}$)

e ($Gd_{0.93}Fe_{2.01}Ni_{0.06}$)

f ($Gd_{1.01}Fe_{1.95}Ni_{0.04}$)

g ($Gd_{1.0}Mn_{2.0}$)

h ($Gd_{0.9}Mn_{2.1}$ – light phase, $K_{0.04}Gd_{0.26}Mn_{0.15}O_{0.55}$ – grey phase)

Fig. 2. SEM images of the electrode materials based on the studied alloys before (a, c, e, g) and after (b, d, f, h) electrochemical hydrogenation (integral composition of the grains is given in parentheses)

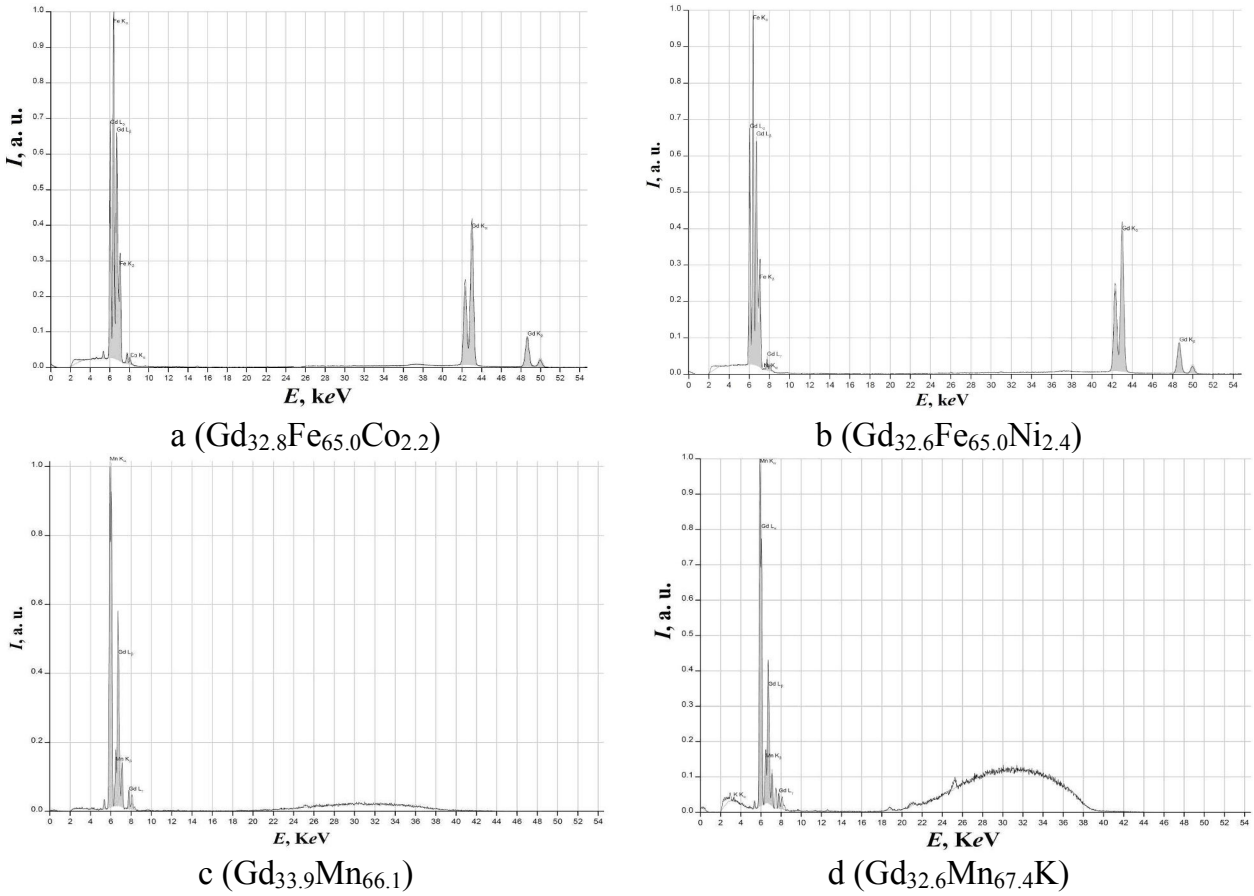

Fig. 3. X-ray fluorescent spectra of $Gd_{33.3}Fe_{64.7}Co_2$ (a) and $Gd_{33.3}Fe_{64.7}Ni_2$ (b) before electrochemical hydrogenation and of $Gd_{33.3}Mn_{66.7}$ before (c) and after 50 cycles (d) of hydrogenation (integral composition of the powdered samples are given in parentheses)

$GdFe_{2-x}Co_x$ and $GdFe_{2-x}Ni_x$ before 50 cycles of the electrochemical hydrogenation was determined by X-ray fluorescence spectroscopy (Fig. 3,a,b). The results are similar to the data obtained from EDX-analysis of powdered samples. In case of $GdMn_2$, the leaching of Gd during electrochemical processes is more significant, that is why we observed a decrease in the Gd-content in the sample (Fig. 3, c,d). Integral composition and mapping of the elements for $GdMn_2$ electrode doped with Zn or Fe has confirmed the nominal composition of the samples (Fig. 4). A trace amount of Gd-based solid solution observed by EDX and XRD methods did not affect electrochemical properties of the samples. In all cases, the results of X-ray powder diffraction were in good agreement with those of energy dispersive X-ray analysis and X-ray fluorescent spectroscopy.

Electrochemical hydrogenation of the phases

The efficiency of electrochemical hydrogenation of the binary intermetallic compounds $GdFe_2$ and $GdMn_2$ and the influence of the alloying components (Mn, Co, Ni, Zn and Mg) on the electrochemical hydrogenation of the phases were studied in this research. Some delected charge-discharge curves for battery prototype with above-mentioned electrode materials are shown in Figs. 5 and 6. The numbering in these Figures specifies the number of charge-discharge cycles. The charge curves illustrate electrochemical processes and side effects that occur at battery charging. For example, at the beginning of hydrogenation, we observed the formation of solid electrolyte interface (Fig. 5,a) that is pointed as small potential jump which disappeared at passing current. This by-reaction has promoted the etching of electrode surface and a decrease in the electrode capacity. Figure 5,b demonstrates the typical charge dependence for the samples $GdMn_{2-x}Ni_x$. Increasing the charge plateau depends on the passivation of the grains surfaces that is undesirable and causes the energy loss. The discharge time and the nominal value of plateau potential were different for each of the electrodes. A decrease in discharge time and H-sorption after 30th cycle can be explained by significant amorphization of the electrode materials.

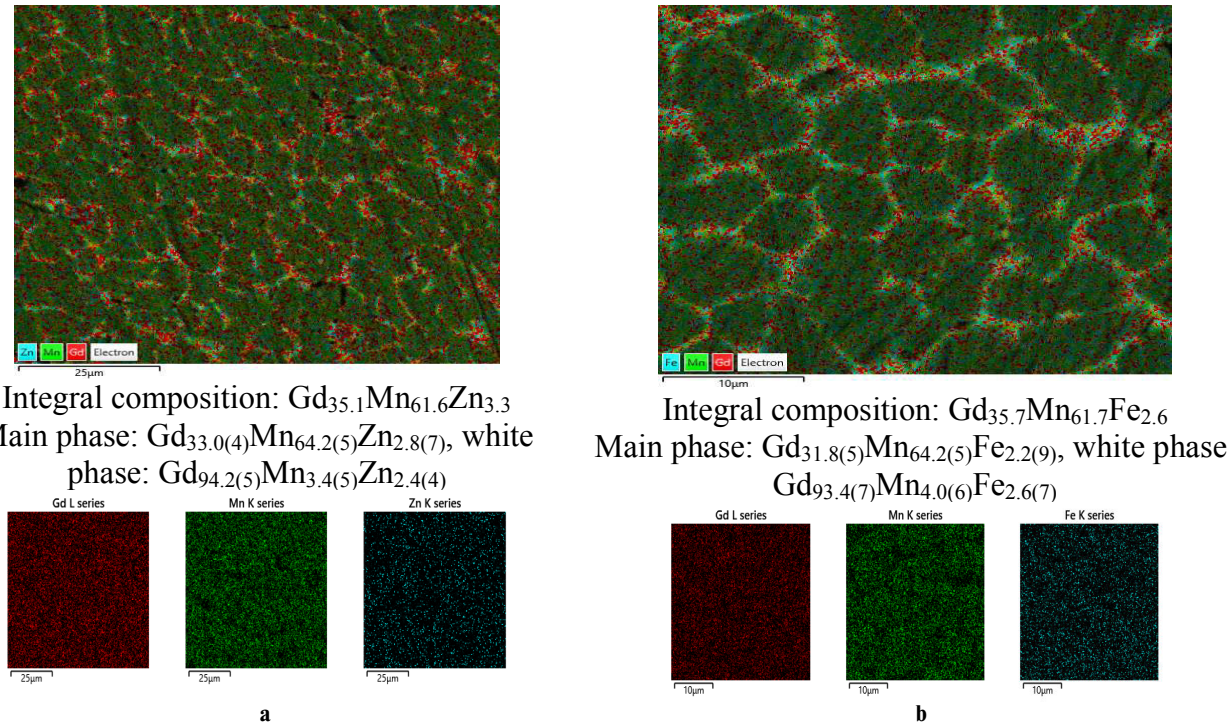

Fig. 4. SEM images (BSE-detector) and elemental mapping of $Gd_{33.3}Mn_{64.7}Zn_2$ (a) and $Gd_{33.3}Mn_{64.7}Fe_2$ (b) electrode materials

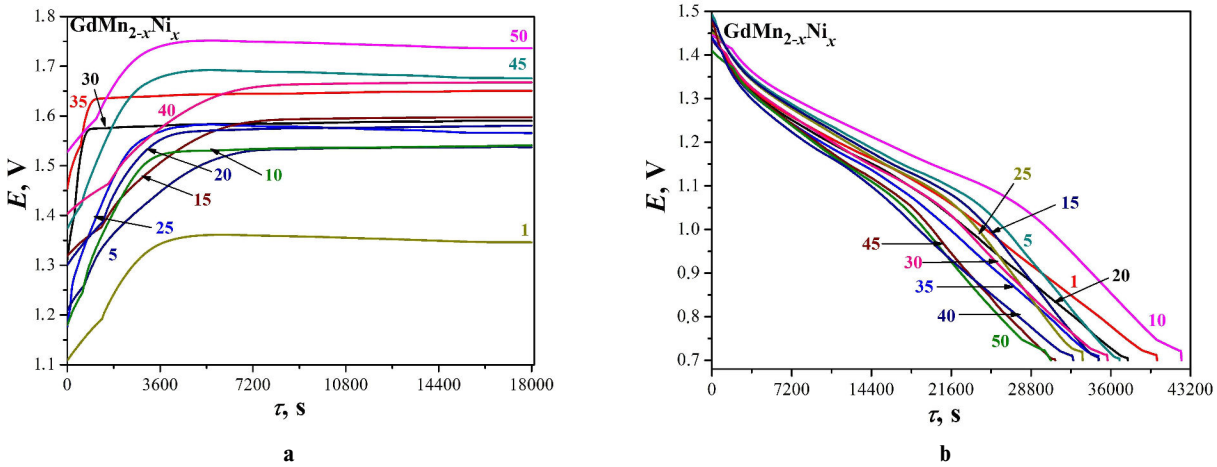

Fig. 5. Selected charge (a) discharge (b) curves for battery prototype with electrodes based on $GdMn_{2-x}Ni_x$

The potential of the plateau depends on physical and chemical characteristics of the material and each of the components, in particular while the discharge time depends on the structural characteristics of matrix and hydrogen mobility in the solid state. Under experimental conditions, the amount of desorbed hydrogen during discharging of the batteries increased in the following series Zn<Mn<Mg<Co<Ni and Zn<Fe<Mg<Co<Ni for $GdFe_{2-x}M_x$ and $GdMn_{2-x}M_x$, respectively. For example, this value is 0.023 H/f.u. and 0.020 H/f.u. for the anode materials based on $GdFe_2$ and $GdMn_2$, respectively. Doping of the binary phases with Zn gave the value of 0.027 H/f.u. for $GdFe_{2-x}Zn_x$ and 0.025 H/f.u. for $GdMn_{2-x}Zn_x$. Among the electrodes based on $GdFe_{2-x}M_x$, the best result on hydrogen capacity 0.047 H/f.u., 0.054 H/f.u. and 0.061 H/f.u. demonstrated the samples doped with Mg, Co and Ni, respectively. The $GdMn_{2-x}M_x$-based electrodes showed a similar behavior, so the highest value of hydrogen capacity 0.049 H/f.u., 0.067 H/f.u. and 0.081 H/f.u. gave the samples doped with the same components Mg, Co and Ni, correspondingly. The electrode based on $GdFe_{1.94}Mn_{0.06}$ showed the amount of desorbed hydrogen of 0.044 H/f.u. and that based on the inverted composition $GdMn_{1.94}Fe_{0.06}$ gave

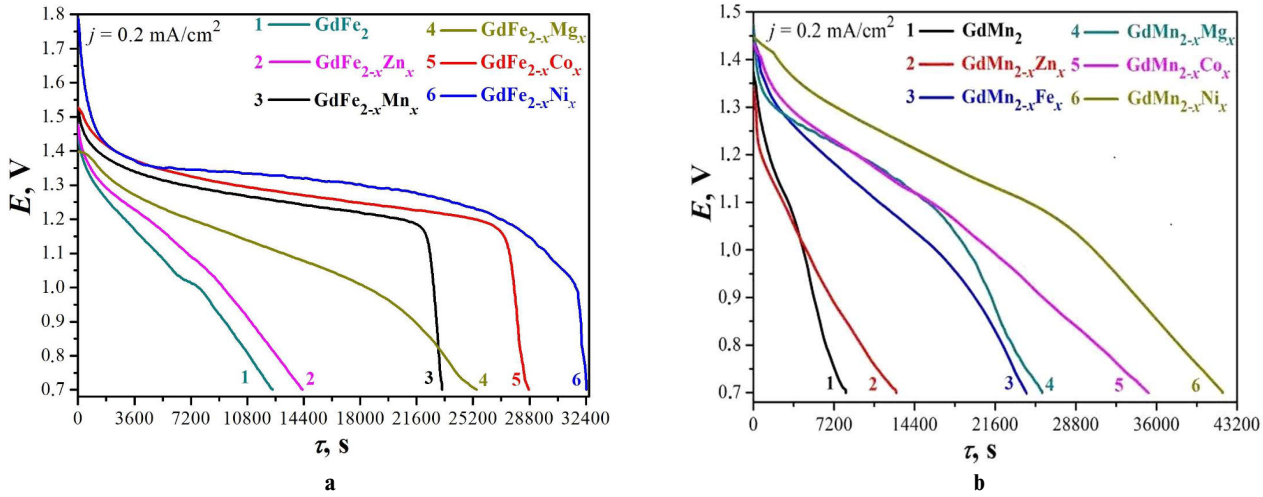

Fig. 6. Selected discharge curves (10th cycle) for batteries prototype with electrodes based on $GdFe_{2-x}M_x$ (a) and $GdMn_{2-x}M_x$ (b)

slightly higher value of 0.047 H/f.u. In general, both series of solid solutions as electrode materials are characterized by a similar effect of alloying additives, including stability in the electrolyte medium and reduction of potential barriers, on the mobility of hydrogen in the volume of solids. The selected discharge curves for two investigated series of alloys on the 10th cycle, when the activation processes on the surface of the grains and in the volume of the electrodes were completed, are shown in Fig. 6. Potential of plateau is the highest for Mn-, Co- and Ni-doped electrodes of the $GdFe_{2-x}M_x$ series and is in the range of 1.07−1.38 V. In the case of $GdMn_{2-x}M_x$ electrode, the highest potential of plateau is observed for Mg-, Co-, and Ni-doped samples (0.98−1.35 V). If the potential (nominal voltage) is higher, the specific energy consumption of the material is larger. The electrodes with Mg, Co and Ni showed improved cyclic stability and no evidences of significant oxidation, while the formation of oxides ZnO and Gd_2O_3 during hydrogenation was detected for the electrode with Zn by XRD and EDX analyses. We observed similar electrochemical behavior earlier during hydrogenation of the phase with a high content of Zn, namely $LaZn_{5-x}Mn_x$ [15].

Corrosion stability of electrodes

The cyclic voltammogram does not show evidences of molecular hydrogen evolution in the cathode area and oxygen in the anode area of the studied samples contacting with an electrolyte in the potential range of −1.6 V to +1.6 V. The polarization curves obtained by logarithmizing the current values show the real range of electrode stability. The battery prototype with $GdFe_2$-based electrode demonstrates stability in a three-electrode cell (Pt reference electrode), which is confirmed by cyclic and linear voltammetry curves (Fig. 7,a,b). The last indicate that corrosion potential is −0.162 V. In the area of more negative potentials, we observed the active corrosion processes.

The Nyquist diagram (Fig. 7,e) shows a semicircle, which characterizes the presence of one electrochemically active phase. In the case of electrode material doped with Ni, we observed the shift of the corrosion potential to the cathode area with more negative potentials (E_{cor}=−0.695 V) (Fig. 7,c,d). In addition, the range of corrosion stability is larger than that for the binary electrode (−0.650 V ... +0.750 V). Since the alloy $Gd_{33.3}Fe_{64.7}Ni_2$ contains a trace amount of $GdFe_3$ (structure type $PuNi_3$, space group R-3m), which also demonstrates electrochemical activity, we can see two semicircles and two maximums in the Nyquist diagram (Fig. 7, f). The shape of EIS dependences of the ternary electrode explains better diffusion of hydrogen in the solid phase volume.

Previous studies on the hydrogenation of R−M−M' intermetallic compounds showed that the octahedral voids formed by are-earth and transition metal atoms and tetrahedral voids formed by transition metal atoms are the most suitable for hydrogen insertion. During the hydrogenation of $GdFe_{2-x}M_x$ and $GdMn_{2-x}M_x$ phases, the tetrahedral voids with a Wyckoff position 8a (0 0 0) are the most suitable sites for hydrogen, because this is the only type of voids present in Laves phases with the $MgCu_2$-type structure [13]. Interatomic distances between the atoms of transition metal and hydrogen exceeds 1.6 Å that provides a good mobility of H-atoms into the structure of the phases.

Electrochemical lithiation and sodiation of the phases

The electrochemical lithiation and sodiation

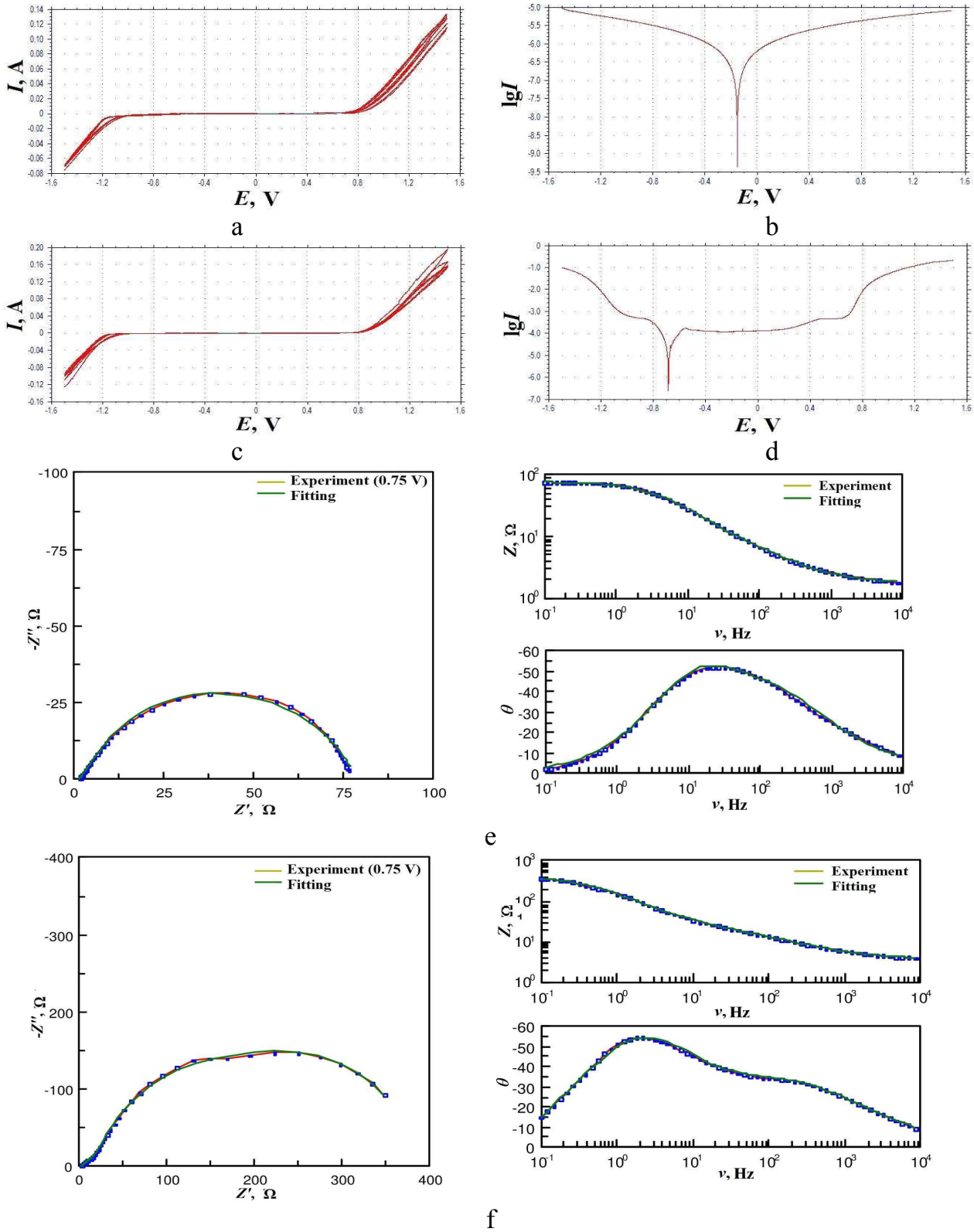

Fig. 7. Cyclic voltammetry curves for the electrodes based on $GdFe_2$ (a) and $GdFe_{1.94}Ni_{0.06}$ (b); linear voltammetry curves for $GdFe_2$ (c), $GdFe_{1.94}Ni_{0.06}$ (d); and EIS dependences for $GdFe_2$ (e) and $GdFe_{1.94}Ni_{0.06}$ (f)

at a low current density (0.1 mA cm^{-2}) was carried out for detailed investigation of electrochemical reactions of $GdFe_{2-x}Zn_x$ and $GdMn_{2-x}Zn_x$ with lithium and sodium at room temperature. No insertion of lithium or sodium into the structural voids was observed during the lithiation and sodiation of $GdFe_{2-x}M_x$ and $GdMn_{2-x}M_x$ phases. The atoms of M-component (Zn) in the structure are replaced by lithium, and the atoms of Gd are replaced by sodium. This difference in interaction is due to the different values in atomic sizes of the elements. The unit cell parameters of the phases before and after lithiation and sodiation are listed in Table 2. As an example, the galvanostatic charge/discharge cycles are given for Mn-containing alloys (Fig. 8), which have improved electrochemical activity as compared with the alloys containing Fe. The electrochemical lithiation and sodiation of the phases can be described by following reactions:

$$GdFe_{2-x}Zn_x + 2yLi^+ + 2y\bar{e} \underset{\text{discharge}}{\overset{\text{charge}}{\rightleftarrows}} GdFe_{2-x}Zn_{x-y}Li_y + yLiZn,$$

$$GdFe_{2-x}Zn_x + 2yNa^+ + 2y\bar{e} \underset{\text{discharge}}{\overset{\text{charge}}{\rightleftarrows}} Gd_{1-y}Na_yFe_{2-x}Zn_x + yGdZn.$$

Conclusions

A clear dependence of the unit cell volume on the atomic radii of doping components was observed for both solid solutions $GdFe_{2-x}M_x$ and $GdMn_{2-x}M_x$ (M=Mn, Co, Ni, Zn, and Mg). In the case of Mg as a dopant, the covalent radii is more suitable for better correlation. The solid solutions based on $GdFe_2$ and $GdMn_2$ with 2 at.% of Co, Ni and Mg as dopants demonstrated better hydrogen sorption properties than those with Mn and Zn. The tetrahedral voids 8a of the $MgCu_2$-type structure are the most suitable sites for hydrogen atoms. Under the same experimental conditions, the capacity parameters increased in the following series: Zn<Mn<Mg<Co<Ni and Zn<Fe<Mg<Co<Ni for the electrodes based on $GdFe_{2-x}M_x$ and $GdMn_{2-x}M_x$, respectively. After 50 cycles of charge/discharge, we observed the changes in the surface morphology and composition of the electrode materials. The corrosion resistance of the doped electrodes is better than of their binary

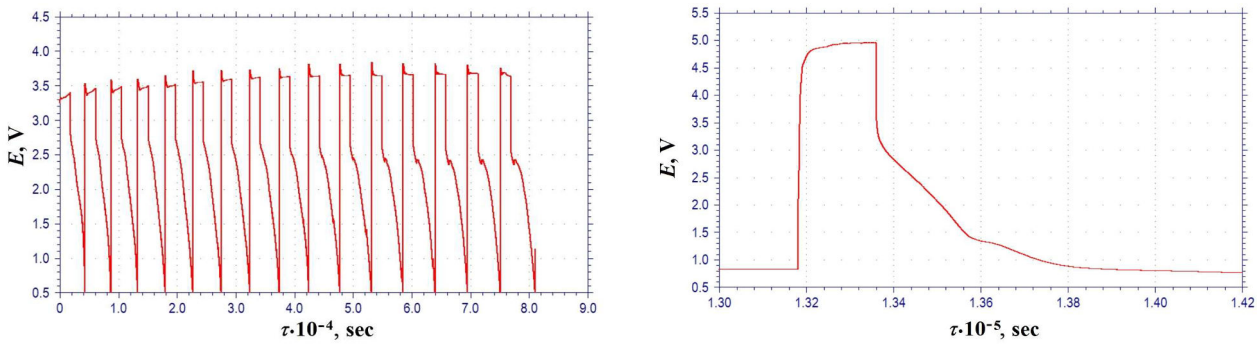

a b

Fig. 8. Galvanostatic charge/discharge cycles of $GdMn_{2-x}Zn_{x-y}Li_y$ (a) and first charge/discharge cycle of $Gd_{1-y}Na_yMn_{2-x}Zn_x$ (b)

Table 2

Unit cell parameters for $GdFe_{2-x}M_x$ and $GdMn_{2-x}M_x$ alloys before and after lithiation and sodiation

Lithiation		Sodiation	
Nominal composition of electrode	Unit cell parameter a, Å	Nominal composition of electrode	Unit cell parameter a, Å
$GdFe_{1.80}Zn_{0.20}$	7.3801(2)	$GdFe_{1.80}Zn_{0.20}$	7.3801(2)
$GdFe_{1.80}Zn_{0.15}Li_{0.05}$	7.3861(4)	$Gd_{0.95}Na_{0.05}Fe_{2-x}Zn_x$	7.3791(5)
$GdFe_{1.80}Zn_{0.10}Li_{0.10}$	7.3927(5)	$Gd_{0.95}Na_{0.05}Fe_{2-x}Zn_x$	7.3773(5)
$GdFe_{1.80}Zn_{0.05}Li_{0.15}$	7.3991(6)	$Gd_{0.95}Na_{0.05}Fe_{2-x}Zn_x$	7.3765(7)
$GdMn_{1.80}Zn_{0.20}$	7.7563(3)	$GdMn_{1.80}Zn_{0.20}$	7.7563(3)
$GdMn_{1.80}Zn_{0.15}Li_{0.05}$	7.7592(4)	$Gd_{0.95}Na_{0.05}Mn_{2-x}Zn_x$	7.7547(5)
$GdMn_{1.80}Zn_{0.10}Li_{0.10}$	7.7631(6)	$Gd_{0.95}Na_{0.05}Mn_{2-x}Zn_x$	7.7533(6)
$GdMn_{1.80}Zn_{0.05}Li_{0.15}$	7.7693(7)	$Gd_{0.95}Na_{0.05}Mn_{2-x}Zn_x$	7.7521(8)

analogues (e.g. the corrosion potentials of $GdFe_2$-based and $GdFe_{1.96}Ni_{0.04}$-based electrodes are −0.162 V and −0.695 V, respectively). No insertion of lithium or sodium into the structural voids was observed during the lithiation and sodiation of the $GdFe_{2-x}M_x$ and $GdMn_{2-x}M_x$ phases. The atoms of the M-component are replaced by lithium and the atoms of gadolinium in the structure are replaced by sodium; this difference in interaction is due to different values in atomic sizes.

REFERENCES

1. *Structural*, electronic and magnetic properties of ErFeMn and $ErFeMnH_{4.7}$ compounds / Mylswamy S., Drozd V., Liu R.-S., Bagkar N.C., Chou C.C., Sun C.P., Yang H.D., Paul-Boncour V., Marchuk I., Filipek S.M., Sheu H.-S., Jang L.-Y. // New J. Phys. − 2007. − Vol.9. − Article No. 271-282.

2. *Structural* and magnetic transformations in the $GdMn_2H_x$ hydrides / Zukrowski J., Figiel H., Budziak A., Zachariasz P., Fischer G., Dormann E. // J. Magn. Magn. Mater. − 2002. − Vol.238. − P.129-139.

3. *Palasyuk T., Figiel H., Tkacz M.* High pressure studies of $GdMn_2$ and its hydrides // J. Alloys Compd. − 2004. − Vol.375. − No. 1-2. − P.62-66.

4. *Stability* of Mn moments and spin fluctuations in RMn_2 (R: Rare earth) / Wada H., Nakamura H., Yoshimura K., Shiga M., Nakamura Y. // J. Magn. Magn. Mater. − 1987. − Vol.70. − No. 1-3. − P.134-136.

5. *Magnetic* properties of crystalline and amorphous $GdFe_2H_x$ alloys prepared by hydrogenation / Mori K., Onodera H., Aoki K., Masumoto T. // J. Alloys Compd. − 1998. − Vol.270. − No. 1-2. − P.35-41.

6. *Amorphization* of laves phase by electrochemical hydrogenation / de Melo M.A.C., de Souza N.E., Zampronio M.A., Colucci C.C., Alves C.S. // J. Non-Cryst. Solids. − 2006. − Vol.352. − No. 32-35. − P.3714-3717.

7. *Heat* capacity and magnetocaloric effect in polycrystalline and amorphous $GdMn_2$ / Sanchez Marcos J., Rodriguez Fernandez J., Chevalier B., Bobet J.-L., Etourneau J. // J. Magn. Magn. Mater. − 2004. − Vol.272-276. − P.579-580.

8. *Phase* equilibrium of the Gd−Fe−Co system at 873 K / Huang J., Zhong H., Xia X., He W., Zhu Y., Deng Y., Zhuang Y. // J. Alloys Compd. − 2009. − Vol.471. − P.74-77.

9. *Hydrogen* storage properties of $LaMg_4Cu$ / Jiang X., Wu Y., Fu K., Zheng J., Li X. // Intermetallics. − 2018. − Vol.95. − P.73-79.

10. *First-principles* investigation of structural and electronic properties of $MgCu_2$ Laves phase under pressure / Liu Y., Hu W.-C., Li D.-J., Zeng X.-Q., Xu C.S., Yang X.-J. // *Intermetallics.* − 2012. − Vol.31. − P.257-263.

11. *Phase* equilibria in the ternary system Gd−Fe−Zn and electrochemical hydrogenation of the phases / Chorna N., Sagan N., Zelinska O., Kordan V., Zelinskiy A., Pavlyuk V. // Chem. Met. Alloys. − 2018. − Vol.11. − No. 1/2. − P.27-33.

12. *King G., Schwarzenbach D.* Latcon. Xtal 3.7 System. − University of Western Australia, 2000.

13. *Electrochemical* hydrogenation of $Mg_{76}Li_{12}Al_{12}$ solid solution phase / Pavlyuk V., Ciesielski W., Pavlyuk N., Kulawik D., Szyrej M., Rozdzynska-Kielbik B., Kordan V. // Ionics. − 2019. − Vol.25. − No. 6. − P.2701-2709.

14. *Hydrogenation* and structural properties of $Mg_{100-2x}Li_xAl_x$ (x=12) limited solid solution / Pavlyuk V., Ciesielski W., Pavlyuk N., Kulawik D., Kowalczyk G., Balinska A., Szyrej M., Rozdzynska-Kielbik B., Folentarska A., Kordan V. // Mater. Chem. Phys. − 2019. − Vol.223. − P.503-511.

15. *Krystalichna* struktura ta elektrokhimichne hidruvannia fazy $LaZn_{5-x}Mn_x$ / Chorna N., Andrash V., Zelinska O., Kordan V., Zelinskiy A., Pavlyuk V. // Visnyk Lviv. Univ., Ser. Khim. − 2018. − Vol.59. − No. 1. − P.107-114.

Received 09.01.2021

ЕЛЕКТРОХІМІЧНЕ ГІДРУВАННЯ, ЛІТІЮВАННЯ І НАТРІЮВАННЯ ІНТЕРМЕТАЛІДІВ $GdFe_{2-x}M_x$ ТА $GdMn_{2-x}M_x$

Н.О. Чорна, В.М. Кордан, А.М. Михайлевич, О.Я. Зелінська, А.В. Зелінський, К. Клузяк, Р.Я. Серкіз, В.В. Павлюк

Електрохімічне гідрування, літіювання та натріювання фаз $GdFe_{2-x}M_x$ та $GdMn_{2-x}M_x$ (M=Zn, Ni, Co, Mn, Mg) та вплив легуючих компонентів на електрохімічні характеристики електродних матеріалів на їхній основі вивчались за допомогою рентгенівської порошкової дифракції, скануючої електронної мікроскопії, енергодисперсійної рентгенівської спектроскопії, рентгенівської флуоресцентної спектроскопії, циклічної вольтамперометрії та електрохімічної імпедансної спектроскопії. Фазовий аналіз вказав на відповідність між параметрами елементарної комірки фаз та атомним радіусом легуючих елементів. Електродні матеріали на основі $GdFe_2$ та $GdMn_2$, леговані 2 ат.% Co, Ni та Mg, продемонстрували кращі гідрогенсорбційні властивості, ніж леговані Mn і Zn. Корозійна стійкість легованих електродів вища, ніж бінарних аналогів (зокрема, потенціал корозії для електрода на основі $GdFe_2$ становить −0,162 В, тоді як для $GdFe_{1,96}Ni_{0,04}$ становить −0,695 В). Ємнісні характеристики збільшуються в ряду Zn<Mn<Mg<Co<Ni для $GdFe_{2-x}M_x$ та в ряду Zn<Fe<Mg<Co<Ni для $GdMn_{2-x}M_x$. Після 50 циклів заряду/розряду спостерігали зміну морфології поверхні та складу електродних матеріалів. У структурі досліджених фаз Лавеса структурного типу $MgCu_2$ найбільш придатними для впровадження атомів водню є тетраедричні пустоти 8*a*. При літіюванні та натріюванні фаз атоми літію заміщують атоми М-компонента в структурі, а атоми натрію заміщують атоми гадолінію. Ця різниця у взаємодії обумовлена різними розмірами атомів. Включення атомів літію чи натрію у структурні пустоти фаз не спостерігалося.

Ключові слова: твердий розчин, електрохімічне гідрування, літіювання та натріювання, нікель-металогідридний акумулятор, літій-іонний акумулятор, натрій-іонний акумулятор.

ELECTROCHEMICAL HYDROGENATION, LITHIATION AND SODIATION OF THE $GdFe_{2-x}M_x$ AND $GdMn_{2-x}M_x$ INTERMETALLICS

N.O. Chorna [a], V.M. Kordan [a], A.M. Mykhailevych [a], O.Ya. Zelinska [a], A.V. Zelinskiy [a], K. Kluziak [b], R.Ya. Serkiz [a], V.V. Pavlyuk [a, b, *]

[a] Ivan Franko National University of Lviv, Lviv, Ukraine

[b] Jan Długosz University of Czestochowa, Czestochowa, Poland

[*] e-mail: volodymyr.pavlyuk@lnu.edu.ua

Electrochemical hydrogenation, lithiation and sodiation of the phases $GdFe_{2-x}M_x$ and $GdMn_{2-x}M_x$ (M=Mn, Co, Ni, Zn, and Mg) and the influence of doping components on electrochemical characteristics of electrode materials on their basis were studied using X-ray powder diffraction method, scanning electron microscopy, energy dispersive X-ray analysis, X-ray fluorescent spectroscopy, cyclic voltammetry and electrochemical impedance spectroscopy. Phase analysis showed a simple correspondence between unit cell parameters of the phases and atomic radii of doping elements. Electrode materials based on $GdFe_2$ and $GdMn_2$ doped with 2 at.% of Co, Ni and Mg demonstrated better hydrogen sorption properties than those doped with Mn and Zn. Corrosion resistance of the doped electrodes was also better than of the binary analogues (e.g. corrosion potential of the $GdFe_2$-based electrode was −0.162 V whereas that of $GdFe_{1.96}Ni_{0.04}$ was −0.695 V). The capacity parameters were increased in the following ranges: Zn<Mn<Mg<Co<Ni and Zn<Fe<Mg<Co<Ni for $GdFe_{2-x}M_x$ and $GdMn_{2-x}M_x$, respectively. After fifty cycles of charge/discharge, we observed the changes in surface morphology and composition of the electrode samples. In the structure of studied Laves type phases with $MgCu_2$-type structure, the most suitable sites for hydrogen atoms are tetrahedral voids 8*a*. During lithiation and sodiation of the phases, the atoms of the M-component of the structure are replaced by the atoms of lithium, and the atoms of gadolinium are replaced by the atoms of sodium. This difference in interaction is due to the difference in atomic sizes of the atoms. No insertion of lithium or sodium into the structural voids of the phases was observed.

Keywords: solid solution; electrochemical hydrogenation; lithiation and sodiation; Ni-MH battery; Li-ion battery; Na-ion battery.

REFERENCES

1. Mylswamy S, Drozd V, Liu RS, Bagkar NC, Chou CC, Sun CP, et al. Structural, electronic and magnetic properties of ErFeMn and $ErFeMnH_{4.7}$ compounds. *New J Phys.* 2007; 9: 271. doi: 10.1088/1367-2630/9/8/271.

2. Zukrowski J, Figiel H, Budziak A, Zachariasz P, Fischer G, Dormann E. Structural and magnetic transformations in the $GdMn_2H_x$ hydrides. *J Magn Magn Mater.* 2002; 238: 129-139. doi: 10.1016/S0304-8853(01)00825-3.

3. Palasyuk T, Figiel H, Tkacz M. High pressure studies of $GdMn_2$ and its hydrides. *J Alloys Compd.* 2004; 375: 62-66. doi: 10.1016/j.jallcom.2003.11.131.

4. Wada H, Nakamura H, Yoshimura K, Shiga M, Nakamura Y. Stability of Mn moments and spin fluctuations in RMn_2 (R: Rare earth). *J Magn Magn Mater.* 1987; 70: 134-136. doi: 10.1016/0304-8853(87)90380-5.

5. Mori K, Onodera H, Aoki K, Masumoto T. Magnetic properties of crystalline and amorphous $GdFe_2H_x$ alloys prepared by hydrogenation. *J Alloys Compd.* 1998; 270: 35-41. doi: 10.1016/S0925-8388(98)00355-7.

6. de Melo MAC., de Souza NE, Zampronio MA, Colucci CC, Alves CS. Amorphization of laves phase by electrochemical hydrogenation. *J Non-Cryst Solids.* 2006; 352: 3714-3717. doi: 10.1016/j.jnoncrysol.2006.03.102.

7. Sanchez Marcos J, Rodriguez Fernandez J, Chevalier B, Bobet JL, Etourneau J. Heat capacity and magnetocaloric effect in polycrystalline and amorphous $GdMn_2$. *J Magn Magn Mater.* 2004; 272-276: 579-580. doi: 10.1016/j.jmmm.2003.11.225.

8. Huang J, Zhong H, Xia X, He W, Zhu Y., Deng Y, et al. Phase equilibrium of the Gd−Fe−Co system at 873 K. *J Alloys Compd.* 2009; 471: 74-77. doi: 10.1016/j.jallcom.2008.03.065.

9. Jiang X, Wu Y, Fu K, Zheng J, Li X. Hydrogen storage properties of $LaMg_4Cu$. *Intermetallics.* 2018; 95: 73-79. doi: 10.1016/j.intermet.2018.01.015.

10. Liu Y, Hu WC, Li DJ, Zeng XQ, Xu CS, Yang XJ. First-principles investigation of structural and electronic properties of $MgCu_2$ Laves phase under pressure. *Intermetallics.* 2012; 31: 257-263. doi: 10.1016/j.intermet.2012.07.017.

11. Chorna N, Sagan N, Zelinska O, Kordan V, Zelinskiy A, Pavlyuk V. Phase equilibria in the ternary system Gd−Fe−Zn and electrochemical hydrogenation of the phases. *Chem Met Alloys.* 2018; 11: 27-33. Available from: http://chemetal-journal.org/ejournal23/CMA0381.pdf.

12. King G, Schwarzenbach D. *Latcon. Xtal 3.7 System.* University of Western Australia, 2000.

13. Pavlyuk V, Ciesielski W, Pavlyuk N, Kulawik D, Szyrej M, Rozdzynska-Kielbik B, et al. Electrochemical hydrogenation of $Mg_{76}Li_{12}Al_{12}$ solid solution phase. *Ionics.* 2019; 25: 2701-2709. doi: 10.1007/s11581-018-2743-8.

14. Pavlyuk V, Ciesielski W, Pavlyuk N, Kulawik D, Kowalczyk G, Balinska A, et al. Hydrogenation and structural properties of $Mg_{100-2x}Li_xAl_x$ (x=12) limited solid solution. *Mater Chem Phys.* 2019; 223: 503-511. doi: 10.1016/j.matchemphys.2018.11.007.

15. Chorna N, Andrash V, Zelinska O, Kordan V, Zelinskiy A, Pavlyuk V. Krystalichna struktura ta elektrokhimichne hidruvannia fazy $LaZn_{5-x}Mn_x$ [Crystal structure and electrochemical hydrogenation of the phase $LaZn_{5-x}Mn_x$]. *Visnyk Lvivskoho Universytetu. Seriia Khimichna.* 2018; 59(1): 107-114. (*in Ukrainian*). doi: 10.30970/vch.5901.107.